Complex and Charge Transfer between TiO_2 and Pyrroloquinoline Quinone†

Nada M. Dimitrijevic,* Oleg G. Poluektov, Zoran V. Saponjic, and Tijana Rajh

Chemistry Division, Argonne National Laboratory, Argonne, Illinois 60439

Received: July 14, 2006; In Final Form: September 5, 2006

Pyrroloquinoline quinone (PQQ) forms a tridentate complex with coordinatively unsaturated titanium atoms on the surface of ~4.5 nm TiO_2 particles; an association constant of $K = 550\ M^{-1}$ per $Ti(IV)_{surf}$ has been determined. Low-temperature electron paramagnetic resonance was employed in identification of localized charges and consequently produced radicals and in determination of charge-transfer processes. The photoexcitation of the PQQ−TiO_2 complex results in the transfer of conduction band electrons from TiO_2 to bound PQQ and the formation of the semiquinone radical. Attaching dopamine (DA) as an electron donor and PQQ as an electron acceptor on the surface of TiO_2 results in spatial separation of photogenerated charges; the holes localize on dopamine and electrons on PQQ, with higher yields than for each component separately. In this triad-type assembly (PQQ−TiO_2/DA) the PQQ that is bound to the particles acts as a sink for electrons allowing their almost complete scavenging even at temperature as low as 4 K.

Introduction

The mechanism of semiconductor-assisted photoconversion is based on the principle that particulate semiconductors behave as miniature photoelectrochemical cells.[1] The absorption of ultra-band-gap energy promotes an electron from the valance band to the conduction band, leaving a positively charged hole in the valence band. Most of the charge pairs recombine either radiatively or nonradiatively. A small fraction of the electrons and holes moves to the surface and either reacts by direct electron transfer with an adsorbed compounds or migrates into midgap surface sites.[2] Surface-trapped charges can also recombine or participate in redox reactions. Although nanoparticulate TiO_2 is very effective from an energetic point of view, it is a relatively inefficient photocatalyst. The main energy loss is due to the recombination of charges generated upon excitation of TiO_2, which is manifested as the relatively low efficiency of long-lived charge separation. In addition, because of its large band gap ($E_g = 3.2$ eV), TiO_2 absorbs less than 5% of the available solar light photons. Hence, the main focus of research for the application of TiO_2 photocatalysis is to improve both the separation of charges and the response in the visible spectral region. Our approach to achieving enlarged separation distances is to employ reconstructed surfaces of TiO_2 nanocrystallites (particles, rods, tubes, and cubes) for obtaining a strong coupling with electron-donating and/or electron-accepting species.[3]

To accommodate the high curvature of TiO_2 in the nanosize regime, the surface reconstructs in such a way that distorts the crystalline environment of surface Ti atoms, changing its coordination from octahedral (bulk) to square-pyramidal (surface), thus forming coordinatively unsaturated Ti atoms at the surface. [4] These surface Ti atoms are very reactive and act as traps for photogenerated charges.[5] We have reported on a whole class of electron-donating enediol ligands that bind to coordinatively unsaturated Ti atoms adjusting their coordination to octahedral geometry at the surface of nanocrystallites and at the same time changing the electronic properties of TiO_2.[4] In these hybrid structures localized orbitals of surface-attached ligands, such as dopamine, are electronically coupled with the delocalized electron levels from the conduction band of a TiO_2 semiconductor. As a consequence of this conformation, absorption of light by the TiO_2/dopamine (TiO_2/DA) system yields the excitation of electrons from the chelating ligand directly into the conduction band of TiO_2 nanocrystallites. This results in a red shift of the semiconductor absorption compared to that of unmodified nanocrystallites and enables harvesting of solar photons. Additionally, this type of electronic coupling yields instantaneous separation of photogenerated charges into two phases, the holes localize on the donating organic modifier, and the electrons delocalize in the conduction band of TiO_2. Moreover, the enediol ligands were found to act as conductive leads, allowing wiring of oligonucleotides and proteins resulting in enhanced charge separation and ensuing chemical transformations.[6,7]

Coupling electron-accepting biomolecules onto the surface of TiO_2 to use them as conductive leads for electrons is a further step toward achieving stabilization of separated charges analogous to supramolecular triads.[8,9] As the electron acceptor we have chosen pyrroloquinoline quinone (PQQ) because it provides several binding sites for metal cations[10−13] and because the redox potential for the reduction of PQQ (~0.1 V vs NHE) is more positive than the flatband potential of TiO_2.[14] The presence of coordinatively unsaturated Ti(IV) atoms on the surface of particles may provide centers for the attachment of PQQ onto TiO_2 nanocrystallites and promote electron transfer from TiO_2 to PQQ. Pyrroloquinoline quinone is a cofactor of various quinoproteins (methanol or glucose dehydrogenases),[15] acting as a redox relay in enzyme catalysis. Without the apoenzyme, PQQ is chemically active, capable of catalyzing different redox reactions and has been used as the redox mediator in the photochemical reduction of CO_2[16] and in the construction of biofuel cells.[14b] In this paper we describe the coupling of PQQ onto the TiO_2 surface and the light-induced charge separation and interfacial electron transfer that extends from the pyrroloquinoline quinone−TiO_2/dopamine (PQQ-TiO_2/DA) triad.

† Part of the special issue "Arthur J. Nozik Festschrift".

* Author to whom correspondence should be addressed. E-mail: dimitrijevic@anl.gov.

10.1021/jp064469d CCC: $33.50
Published on Web 10/21/2006

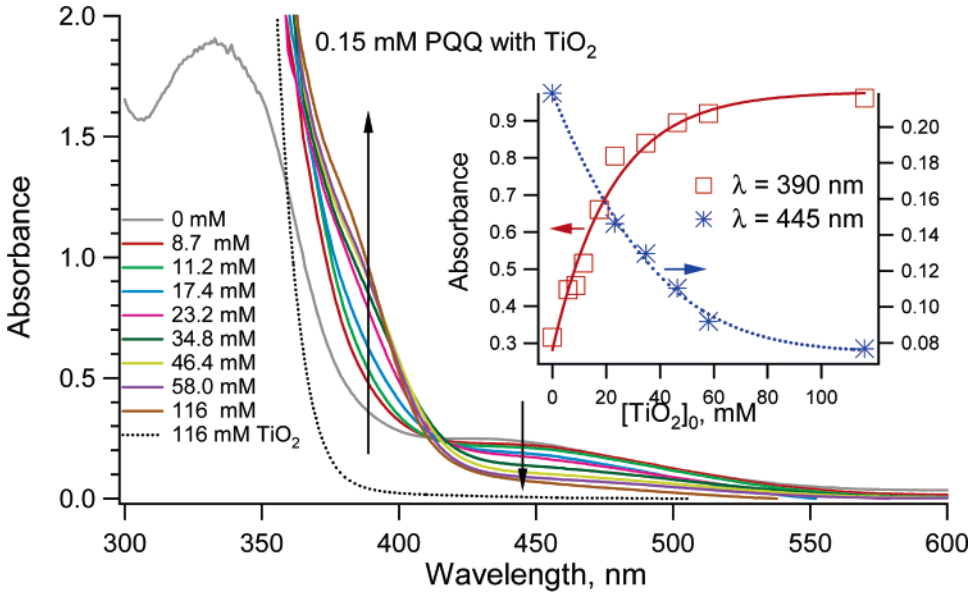

Figure 1. Changes in absorption spectra due to the formation of PQQ−TiO_2 complex. Solution of 0.150 mM PQQ in DMSO containing 0 (gray line), 8.7, 11.2, 17.4, 23.2, 34.8, 46.4, 58, and 116 mM TiO_2. Dotted line is the spectrum of 116 mM TiO_2 in DMSO (highest concentration of TiO_2 used). All solutions contain 10 vol % of H_2O. The optical path length is 1 cm. Inset: Changes in 390 and 445 nm absorbance with increasing concentrations of TiO_2 particles.

Experimental Section

All of the reagents were analytical grade and used as received, without further purification. PQQ was purchased from Sigma. Dimethyl sulfoxide (DMSO) or Milli-Q deionized water (resistivity 18.2 MΩ cm^{-1}) were used as solvents. The titania particles used in this work were 42.8 ± 3.5 Å in diameter. The synthesis and characterization of TiO_2 nanoparticles are described elsewhere.[17]

X-band electron paramagnetic resonance (EPR) experiments were conducted on a Bruker ESP300E spectrometer equipped with a Varian cavity and a variable-temperature cryostat (Air Products). The microwave frequency was measured using a Hewlett-Packard 5352B frequency counter. High-field/high-frequency EPR measurements were performed on a pulsed/continuous wave HF D-band (130 GHz/4.6T) spectrometer as described previously.[18] The *g*-tensors were calibrated for homogeneity and accuracy by comparison to a coal standard, $g = 2.00285 \pm 0.00005$. The simulation program SIMFONIA from Bruker Instruments was used for simulation of the spectra. X-band EPR experiments were conducted at temperatures from 4 to 100 K, while D-band spectra were measured at 30 K. Samples were excited using a 300 W Xe lamp (ILC). A 370 nm cut-off filter was used to avoid excitation of free PQQ and consequently photochemical reactions of its triplet.[12b]

Fourier transform infrared (FTIR) spectra were measured on a Nicolet 510 Fourier transform infrared spectrophotometer equipped with a Spectra Tech diffuse reflectance accessory. Samples were collected as dry material and measured as 8 wt % in a KBr matrix. Typically 100 scans were performed for each spectrum. The resolution was 4 cm^{-1}. Results are presented as Kubelka−Munk plots. The sample of PQQ−TiO_2 was prepared by mixing aqueous solution of TiO_2 and PQQ and drying at room temperature in nitrogen atmosphere.

The absorption spectra were recorded at room temperature in cells with 0.2 or 1 cm optical path lengths using a Shimadzu UV-1601 UV/vis spectrophotometer.

Results and Discussion

Complex between PQQ and TiO_2 Particles. It has been shown that PQQ has several binding sites capable of chelating metal cations.[10] The 4,5-orthoquinone, 6-pyridine, and 7-carboxylic acid functional groups of PQQ molecules are essential for the binding of metal cations. Divalent ions such as Ca(II), Mg(II), Cu(II), Fe(II), and Zn(II) are known to form a 1:1 complex with isolated PQQ molecules in solution.[11−13] The metal center in these complexes is coordinated to the 7-carboxylate oxygen O(7), 6-pyridine nitrogen N(6), and 5-quinonic oxygen atoms O(5), constituting the tridentate O(7),N(6),O(5) site.[12] However, monovalent cations, Na(I) and K(I), can be chelated both at the tridentate site and at the quinonic bidentate site.[19] We exploited the presence of coordinatively unsaturated Ti(IV) on the surface of nanocrystalline TiO_2 particles for the attachment of PQQ onto particles. Interaction between the semiconductor surface and the surface modifier/chelator such as PQQ can be monitored from the changes in absorption spectra of either colloidal particles or modifiers. We monitored the changes in the absorption spectra of PQQ, keeping its concentration constant, upon addition of TiO_2 particles. Dimethyl sulfoxide was used as a solvent because of the high solubility of PQQ in this solvent, its miscibility with aqueous TiO_2 solution, and the long-term stability of PQQ−TiO_2 complex in a DMSO/H_2O mixture. In addition, the absorption spectrum of TiO_2 is not affected by the presence of DMSO. The results are presented in Figure 1. The spectra revealed the following changes associated with an increasing concentration of TiO_2: a decrease in absorption of PQQ at ~450 nm and the formation of a new band/shoulder at 390 nm, with an isosbestic point at 420 nm. These spectral changes were previously observed for complexes of PQQ with both monovalent (Li, Na, K, etc.) and divalent (Ca, Cu) cations[20] and were attributed to the red shift of the ~330 nm absorption band of PQQ due to the binding of cations through the quinone O(5) position (the electron-withdrawing effect of metallic cations).[12c,19c,20] The increase of a new 390 nm band correlates with the decrease in the PQQ absorption band at 445 nm (Figure 1, inset). These spectroscopic

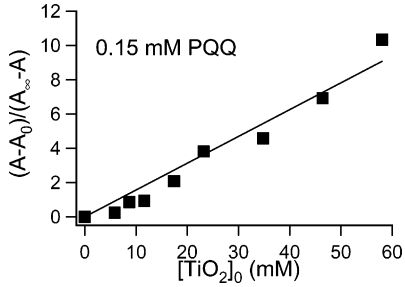

Figure 2. Plot of $(A - A_0)/(A_\infty - A)$ at 390 nm vs $[TiO_2]_0$ concentration for the formation of PQQ−TiO_2 complex. $[PQQ]_0 = 0.15$ mM.

changes reflect the formation of PQQ−TiO_2 complex, eq 1

$$PQQ + TiO_2 \leftrightarrows PQQ{-}TiO_2 \qquad (1)$$

The association constant for the binding of PQQ to TiO_2 particles was determined from the slope in Figure 2, which presents the changes in absorption of a complex as observed at 390 nm with an increased concentration of TiO_2 according to eq 2

$$\frac{A - A_0}{A_\infty - A} = \frac{K}{1 + K[PQQ]_0}[TiO_2]_0 \qquad (2)$$

where $A = \epsilon_{PQQ}[PQQ] + \epsilon_{complex}[PQQ{-}TiO_2]$.

The value of $K = 160\ M^{-1}$ per total titania was determined. Taking into account molar concentration of surface $Ti(IV)_{surf}$, $[Ti(IV)_{surf}] = 12.5[TiO_2]/D$, where D is the diameter of the particles in angstroms, a value for association constant of $K = 550\ M^{-1}$ per $Ti(IV)_{surf}$ is obtained. In comparison to the chelation of Ca(II),[12c] which proceeds both with isolated PQQ and with PQQ in methanol dehydrogenase, the determined binding constant for $Ti(IV)_{surf}$ is only ∼4 times smaller, reflecting a relatively strong binding of PQQ on the surface of TiO_2 particles.

The infrared spectra have further confirmed that $Ti(IV)_{surf}$ binds through O(5) and O(7), most probably forming a tridentate O(5),N(6),O(7) type of complex with PQQ molecules (Figure 3). For measurements of IR spectra, we used a very low concentration of PQQ as compared to TiO_2 particles (1:5) to avoid overlapping of free PQQ absorption. Figure 3 also contains the spectra of bare TiO_2 and free PQQ. Comparison of the IR spectra of bare PQQ and PQQ−TiO_2 complex shows the splitting of the quinone carbonyl band $\nu(C{=}O_{quinone})$ from 1643 cm^{-1} for the free ligand to 1653 and 1636 cm^{-1} in the complex that arises from the coordination of $Ti(IV)_{surf}$ at O(5). At the same time the decrease in the intensity of the $\nu(C{=}O_{ester})$ band accompanied with a slight shift from 1744 cm^{-1} (PQQ) to 1749 cm^{-1} (complex) indicates coordination of surface titanium at O(7) position. The same types of changes in IR spectra are reported for Ca(II) and Cu(II) tridentate O(5),N(6),O(7) complexes with PQQ, which were independently confirmed with X-ray crystallographic and NMR measurements.[10,13] The presence of ester groups in "pure" PQQ, besides carboxylic acid groups, $\nu(C{=}O_{carboxyl})$ observed at 1720, 1703, and 1683 cm^{-1}, suggests that there is a residue from OH protection in the PQQ commercial sample.

Light-Induced Charge Transfer. Excitation of nanocrystalline TiO_2 with photon energies larger than its band gap results in the formation of conduction band electrons and valence band holes, eq 3

$$TiO_2 \xrightarrow{h\nu} (e^-_{CB} + h^+_{VB})TiO_2 \qquad (3)$$

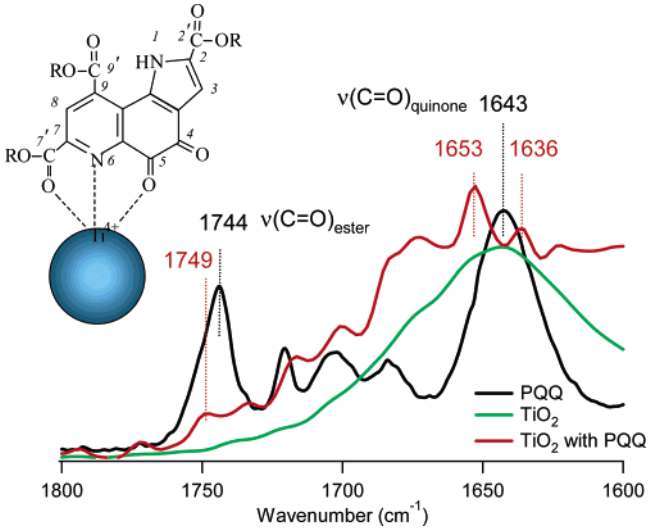

Figure 3. Comparison of the infrared spectra of bare PQQ (black) and PQQ adsorbed on TiO_2 particles (red line). The spectrum of the PQQ−TiO_2 complex is superimposed on the spectrum of bare TiO_2 (green line); the broad band in the region of ∼1650 cm^{-1} is characteristic of adsorbed water bending. Inset: Schematic presentation of the tridentate complex between $Ti(IV)_{surf}$ and PQQ.

Once produced, the charge carriers become trapped into lower-energy states. Localization of conduction band electrons and valence band holes into lower-energy states occurs in less than 30 ps.[21−24] In the presence of electron donors or acceptors attached onto the surface of TiO_2 particles, interfacial charge transfer occurs accompanied by the competition with trapping and recombination of charge carriers. To probe the interfacial charge transfer between photogenerated electrons and PQQ attached to the surfaces of TiO_2 nanoparticles, we studied charge separation, trapping, and transfer using an EPR technique. Low-temperature EPR spectroscopy provides an unambiguous identification of the species involved in the charge separation processes by revealing changes in local symmetry along the pathway of charge carriers, enabling identification of charge trapping sites on TiO_2 as well as radicals formed in the reaction of photogenerated charges with adsorbed molecules.

Our approach in investigating charge-transfer reactions was to use a solution of DMSO (with 16% H_2O) because it provides means for the formation of transparent and stable solutions of both bare TiO_2 particles and complexes of TiO_2 with PQQ and/or dopamine. The stability of transparent solutions enabled control over a range of concentrations, temperatures, and pH values. However, DMSO is an efficient scavenger of oxidizing species.[25,26] When bare TiO_2 particles were suspended in a DMSO/H_2O mixture and exposed to band-gap excitation, the EPR spectra have revealed that DMSO acts as a sacrificial scavenger of photogenerated holes. The four-line spectrum with the intensity ratio of 1:3:3:1, g-tensor of 2.002, and hyperfine splitting constant $a_H = 23$ G is characteristic of $^\bullet CH_3$ radicals[27] (Figure 4a, black line). Thus, methyl radicals are formed in the reaction of surface-trapped holes, $Ti(IV)O^\bullet_{surf}$,[28,29] with DMSO, eqs 4 and 5. At the same time, as can be seen from the EPR spectrum, electrons are localized in the interior of TiO_2 particles. The sharp signal at $g_\perp = 1.988$ and weak parallel signals with $g_{||}^1 = 1.961$ and $g_{||}^2 = 1.958$ correspond to lattice-trapped electrons, $Ti(III)_{latt}$[30,31]

$$h^+_{VB} + Ti(IV)OH_{surf} \rightarrow Ti(IV)O^\bullet_{surf} + H^+ \qquad (4)$$

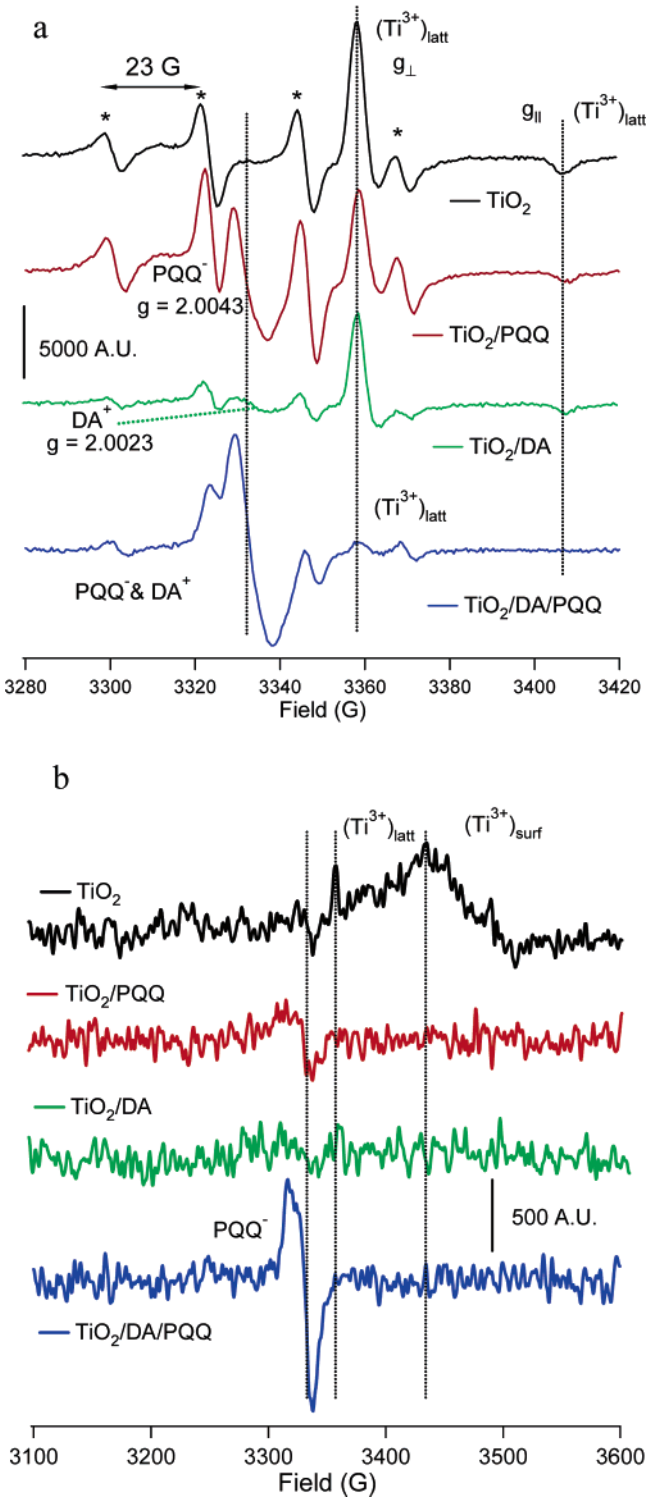

Figure 4. X-band EPR differential spectra: (a) measured at 4.5 K under illumination (370 nm cut-off filter) of unmodified TiO_2 particles (black line TiO_2), TiO_2 modified with PQQ, (red line TiO_2/PQQ), TiO_2 modified with dopamine (green line TiO_2/DA), and TiO_2 particles modified both with PQQ and dopamine (blue line TiO_2/DA/PQQ); (b) measured at 4.5 K in the dark after illumination at 80 K. In all solutions concentrations of participating solutes were kept constant. Solvent: DMSO with 16% H_2O. The concentration of TiO_2 was 46.5 mM in all solutions. The PQQ concentration was 0.15 mM, corresponding to ~5 molecules per TiO_2 particle, and the concentration of dopamine was 0.8 mM (~23 molecules), which results in <2% surface coverage. For better viewing, the four-line signal from the CH_3 radicals is denoted with asterisks.

$$H_3C-S(=O)-CH_3 + Ti(IV)O^{\bullet}_{surf} \xrightarrow{H_2O} {}^{\bullet}CH_3 + H_3C-S(=O)-OH + Ti(IV)OH_{surf} \quad (5)$$

When the PQQ−TiO_2 complex in DMSO was illuminated, the EPR spectra showed a decrease in the intensity of the lattice-trapped $Ti(III)_{latt}$ electrons signal accompanied by the appearance of a new band with $g = 2.0043$ and a slight increase in the intensity of methyl radical signals (Figure 4a, red line). As the EPR spectra were taken under illumination, the intensities of the signals correspond to the steady-state concentrations of products, in our case ruled by the formation and recombination of electrons and holes, and products of their subsequent reactions. Thus, observed changes reflect the transfer of photogenerated electrons from titania particles to PQQ and the formation of the semiquinone radical, eq 6

$$TiO_2(e^-_{CB}) + PQQ \rightarrow PQQ^- \quad (6)$$

The reaction between photogenerated electrons and PQQ was further confirmed illuminating samples at elevated temperature (80 K) and measuring EPR spectra at 4.5 K in the dark (Figure 4b). When the temperature is increased from 4 to 80 K, the electrons from the interior of the bare particle move to the surface where they localize at midgap states. The decrease of the signal for lattice-trapped $Ti(III)_{latt}$ electrons and the increase of the broad signal with $g_\perp = 1.924$ that corresponds to the surface-trapped electrons, $Ti(III)_{surf}$,[32] can be seen for bare TiO_2 (Figure 4b, black line). However, attached PQQ on the surface of the TiO_2 particle acts as a powerful electron acceptor. When the temperature is increased, detrapped lattice electrons do not localize on the surface, but rather they react with PQQ (Figure 4b, red line). As a consequence, no signals due to either lattice- or surface-trapped electrons can be observed; only the signal of the PQQ semiquinone radical is present.

Furthermore we examined the possibility of extended charge separation in a triad-type assembly, having attached dopamine as an electron donor and PQQ as an electron acceptor on TiO_2 particles, PQQ−TiO_2/DA. As mentioned previously dopamine forms an irreversible bidentate complex with surface coordinatively unsaturated titanium atoms (TiO_2/DA) that results in spatial separation of photogenerated charges.[4,33] The complex is so efficient that in DMSO solution even with very low coverage of the surface coordinatively unsaturated sites with dopamine (<2% of possible 405 sites) dopamine relatively successfully competes for photogenerated holes with DMSO. Namely, the intensity (number of spins/concentration) of the signal that corresponds to ${}^{\bullet}CH_3$ radicals is lowered compared to that of the unmodified TiO_2, while the signal from $Ti(III)_{latt}$ electrons is unchanged. Moreover, a weak signal with $g = 2.0023$ that corresponds to oxidized dopamine can be observed from EPR spectra (Figure 4a, green line). The low intensity of DA^+ is due to the low concentration of dopamine and competition with DMSO. Increasing the temperature to 80 K results in recombination of charges in the TiO_2/DA complex, Figure 4b, green line. The presence of both electron donor (DA) and electron acceptor (PQQ) attached to the surface of TiO_2 particles promotes extended charge separation similar to the molecular triads, with separation of charges on different reversible ligands, as can be seen from EPR spectra of the illuminated PQQ−TiO_2/DA complex (Figure 4a, blue line). The signal that corresponds to PQQ^- doubles in intensity compared to that of PQQ−TiO_2 without dopamine, accompanied with the drastic reduction of the $Ti(III)_{latt}$ signal. An increase in temperature has revealed that a significant amount of electrons is stored in PQQ due to

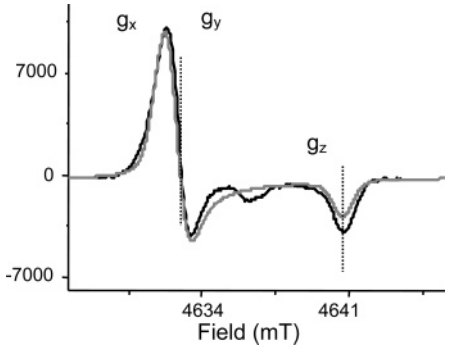

Figure 5. D-band EPR differential spectrum of illuminated PQQ/TiO_2 in DMSO. Temperature 30 K, [TiO_2] = 46.5 mM, [PQQ] = 0.15 mM. The solution contains 16% H_2O. The gray line is a simulated spectrum.

the suppressed charge recombination in this triad (Figure 4b, blue line). Increasing the concentration of dopamine in a PQQ−TiO_2/DA triad increases the efficiency of electron transfer to PQQ (Supporting Information).

To confirm that semiquinone radicals are formed as a result of one-electron reduction of PQQ we performed high-field/high-frequency EPR (130 GHz) measurements. The D-band spectrum of PQQ−TiO_2 under illumination is presented in Figure 5. Although rhombic symmetry of the *g*-tensor is not fully resolved, the principal values of the *g*-tensor can be extracted by the theoretical simulation of the EPR spectrum. The obtained values from theoretical simulation, $g_x = 2.0057$, $g_y = 2.0055$, and $g_z = 2.0019$ with $g_{iso} = 2.0043$, are in agreement with previously reported values for PQQ semiquinone radicals.[34,35]

Effect of Temperature on Charge Transfer. The kinetics of the PQQ semiquinone formation can be exploited for determining the energy levels of lattice trapping sites in TiO_2, since by increasing the temperature electrons from lower-energy sites reach the conduction band and can participate in charge transfer with a surface-attached species. The rate of formation of semiquinone radicals depends on the activation energy for detrapping and/or activation energy of charge-transfer reaction defined by the difference in redox potentials of conduction band electrons and PQQ molecules as well as the reorganization energy of the charge-transfer complex. Nevertheless, in the first approximation, the correlation between the apparent rate of semiquinone formation, k_{obs}, and the activation energy for detrapping, ($E_{CB} - E_{trap}$), can be expressed with eq 7

$$k_{obs} \propto e^{-(E_{CB}-E_{trap})/k_B T} \quad (7)$$

where k_B is the Boltzmann constant, T is the absolute temperature, and E_{CB} and E_{trap} are the conduction band edge and trap energy levels, respectively.[36]

Taking advantage of the long lifetime of localized charges in bare TiO_2, on the order of hundreds of seconds at liquid nitrogen temperature,[37] we measured the rates of formation of PQQ^- radicals by monitoring their signals over a range of temperatures from 4 to 80 K. Figure 6 presents changes in the intensity of the EPR signal measured at static magnetic field that corresponds to the PQQ^- radicals (3329 G) with exposure to light. Kinetic traces for a few representative temperatures are presented.

From the kinetics data presented in Figure 6 two processes are distinguished. At temperatures ≤40 K the fast formation of semiquinone PQQ^- radicals is observed resulting in their relatively low equilibrium/saturation concentration that does not change between 4 and 40 K (Figure 6, inset). The process is characterized by extremely low activation energy $\Delta E < 1$ meV

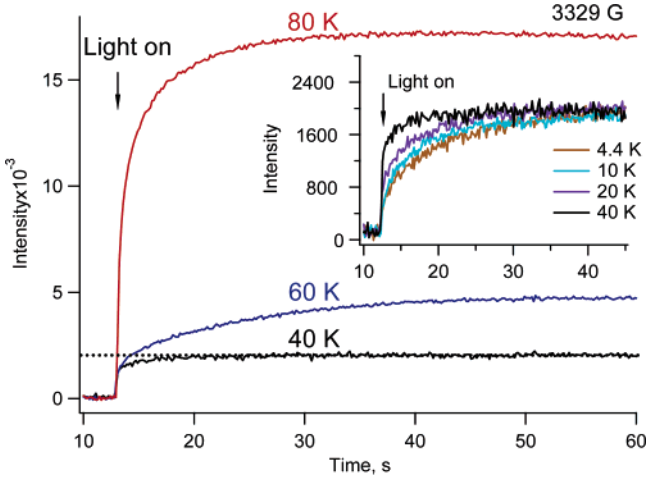

Figure 6. Signals corresponding to the PQQ^- radicals as a function of light exposure for different temperatures (in the range of 4−80 K). The solution is as in Figure 4.

(Supporting Information). Such a low energy suggests that electrons are positioned at states just below the conduction band and that their reaction with PQQ proceeds through electron hopping between equivalent lattice sites. The presence of such states was detected in reduced single-crystal rutile, and the mechanism of hopping accompanied with dipolar reorientation was proposed in explaining a sharp dielectric relaxation in this system at liquid He temperatures.[38] A low concentration and saturation of the PQQ^- signal would indicate a low concentration of these relatively mobile electrons. Another possibility is the reaction of PQQ with conduction band electrons, in which case observed changes in charge-transfer kinetics could result from the electron−phonon coupling.[39] Despite the origin of electrons involved in reaction at temperatures below 40 K, only PQQ molecules that are attached to the surface of the particles can accept electrons. At these temperatures free PQQ molecules in solution cannot diffuse to the surface of the particle and participate in a charge-transfer reaction, and the electrons that are trapped in deeper traps in TiO_2 do not have enough energy to move to the surface, react with adsorbed molecules, or localize at surface trapping sites. If there are no attached electron acceptor molecules on TiO_2, such is the case, for example, for methyl viologen, then no transfer of photogenerated electrons can be observed at these low temperatures in the presence of the sacrificial electron donor, even when the redox potential of viologen favors electron transfer. Only when temperature is elevated, the surface-trapped electrons can react with methyl viologen (Supporting Information). At temperatures >40 K the electrons from the energetically deeper lattice sites detrap to the conduction band and react with PQQ molecules, which can be observed by the increase in concentration of semiquinone radicals as the number of detrapped electrons increases (Figure 6). From the limited range of temperatures examined in this work (up to 100 K) these deeper trapping sites are positioned at least 20 meV below the conduction band (Supporting Information). Studies to determine detailed energetics of lattice deep traps are underway.

Effect of pH on Charge Transfer. The two-step one-electron reduction of quinone to quinol is the dominant reduction pathway for PQQ incorporated into enzymes and for PQQ in aprotic solvents. It was found that the complex of PQQ with Ca(II) inside the enzyme additionally increases stability of the PQQ semiquinone.[11,12] Thermodynamic stability of the semiquinone radical anion is also enhanced in alkaline solution due to the deprotonation, pK = 8.5,[40] which results in localization

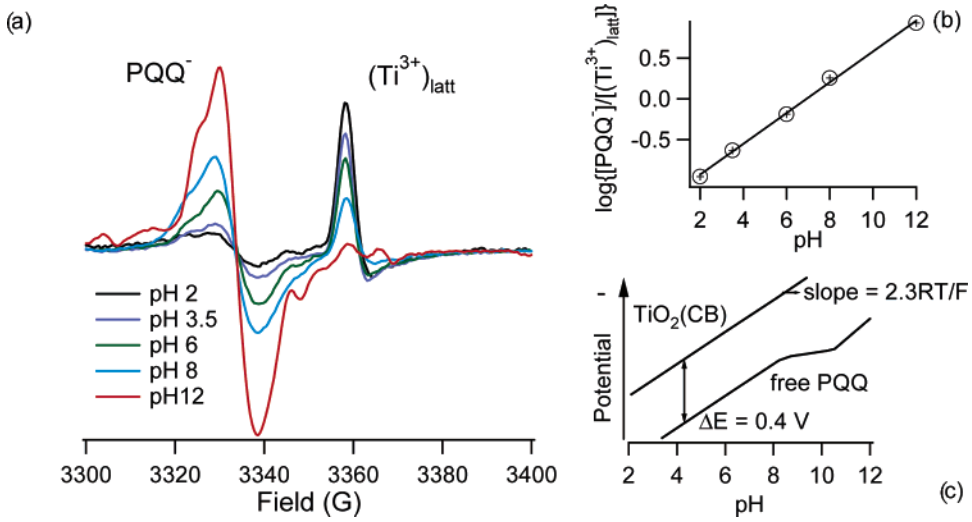

Figure 7. (a) X-band EPR differential spectra of PQQ−TiO_2 complex in DMSO/H_2O mixture under illumination (370 nm cut-off filter) as a function of pH. Temperature 10 K. [TiO_2] = 46.5 mM, [PQQ] = 0.15 mM, and solution contains 16% H_2O at various pH. (b) Ratio of the intensities of semiquinone and localized electron signals as a function of pH. (c) Changes in the potential of the TiO_2 conduction band edge and free PQQ with pH, according to eqs 9 and 11.

of the negative charge and the spin onto the quinone moiety of the PQQ molecule.[12d] We examined the effect of pH on charge transfer between TiO_2 and the attached PQQ to obtain information on the redox properties of the complex and the stability of semiquinone radicals. The pH of TiO_2 was adjusted initially, and nanocrystallites were brought into contact with PQQ solution in DMSO; the final concentrations were 0.15 mM PQQ, 46.5 mM TiO_2, and 16% H_2O. The pH did not affect the association constant of the complex. Figure 7a presents EPR spectra of illuminated PQQ−TiO_2 complexes at various pH values measured at 10 K. As can be seen from Figure 7a, increasing the pH yields an increase of the PQQ^- concentration, while the concentration of $Ti(III)_{latt}$ decreases. The competition between transfer of conduction band electrons to PQQ and their localization in the particle interior controls the ratio of PQQ^- and $Ti(III)_{latt}$ concentrations. The ratio of concentrations, $[PQQ^-]/[Ti(III)_{latt}]$, correlates to the difference in the redox potentials of TiO_2 conduction band (E_{CB}) and that of attached PQQ (E_{PQQ}), eq 8

$$\log\left(\frac{[PQQ^-]}{[Ti(III)_{latt}]}\right) \propto \frac{F}{2.3RT}(E_{CB} - E_{PQQ}) \qquad (8)$$

where F is the Faraday constant, R is the gas constant, and T is the temperature.

Both the E_{CB} of bare titania particles and E_{PQQ} of free PQQ shift to negative values with pH. Equation 9 provides the Nernstian dependence of the conduction band edge of TiO_2 on the pH of solution

$$E_{CB}(pH) = E_{CB}(pH_0) - \frac{2.3RT}{F}pH \qquad (9)$$

However, if one considers the redox and acid−base equillibria of free PQQ in aqueous solution, presented in the following scheme

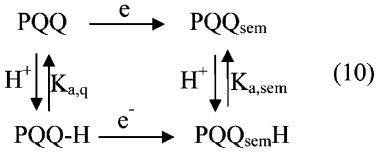

(10)

then the pH dependence of its redox potential is given by eq 11. The values for acid dissociation constants are $pK_{a,sem} = 8.5$ for the phenolic hydroxyl group of semiquinone and $pK_{a,q} = 10.3$ of the pyrrole NH group, respectively.[12d]

$$E_{PQQ}(pH) = E_{PQQ}(pH_0) - \frac{2.3RT}{F}pH + \frac{2.3RT}{F}\log\frac{[H^+] + K_{a,sem}}{[H^+] + K_{a,q}} \qquad (11)$$

For comparison Figure 7c presents the changes in E_{CB} (of bare TiO_2) and E_{PQQ} (of isolated PQQ) with pH according to eqs 9 and 11. If attached PQQ on the surface of TiO_2 particles exhibits the same acid−base equillibria as described with eq 10, then the driving force for charge transfer, $E_{CB} - E_{PQQ}$, would be proportional only to the last term of eq 11. Thus, according to eq 8, $\log([PQQ^-]/[Ti(III)_{latt}])$ will show no dependence on pH, at least to pH 8.5. However, as can be seen from Figure 7b, our results show linear dependence with a slope of $b \approx 0.2$

$$\log\left(\frac{[PQQ^-]}{[Ti(III)_{latt}]}\right) \propto \frac{F}{2.3RT}(E_{CB} - E_{PQQ}) \propto bpH \qquad (12)$$

This result indicates that the PQQ−TiO_2 complex has quite different properties compared to isolated species and is a result of strong electronic coupling of PQQ with titania particles. It has been shown that the type of anchoring groups of attached molecules on TiO_2 do not change the dependence of conduction band edge on pH, but rather it affects density of electronic states and thus interfacial electron-transfer rates.[41] Additionally, binding of PQQ to $Ti(IV)_{surf}$ may affect deprotonation of semiquinone radicals, as was previously observed for some metal cations,[15] causing changes in the redox potential of the attached PQQ.

Conclusion

The presence of coordinatively unsaturated titanium atoms on the surface of TiO_2 particles was exploited for binding electron-donating (dopamine) and electron-accepting (pyrroloquinoline quinone) biomolecules to the titania particles. In this way construction of the nanoparticle triad was achieved. The PQQ−TiO_2/DA triad has unique photoelectrochemical proper-

ties that promote spatial separation of photogenerated charges, holes localized at dopamine and electrons at PQQ. Although both DA and PQQ are reversible ligands, it was found that recombination of charges is suppressed in the nanoparticle triad assembly.

Acknowledgment. The work was performed under the auspices of the U. S. Department of Energy, Office of Basic Energy Sciences, Division of Chemical Sciences, Geosciences and Biosciences, under Contract No. W-31-109-Eng-38.

Supporting Information Available: Effect of dopamine concentration on the efficiency of charge transfer in the PQQ−TiO_2/DA triad, Arrhenius plots for the rates of formation of the PQQ^- semiquinone radical, and the effect of temperature on the EPR signals for PQQ as compared to methyl viologen. This material is available free of charge via the Internet at http://pubs.acs.org.

References and Notes

(1) (a) Hagfeldt, A.; Gratzel, M. *Chem. Rev.* **1995**, *95*, 49. (b) Hoffman, M. R.; Martin, S. T.; Choi, W.; Bahnemann, D. W. *Chem. Rev.* **1995**, *95*, 69. (c) Mills, A.; LeHunte, S. *J. Photochem. Photobiol., A* **1997**, *108*, 1 and references therein.

(2) Nozik, A. J. *Annu. Rev. Phys. Chem.* **1978**, *29*, 189.

(3) (a) Saponjic, Z. V.; Dimitrijevic, N. M.; Tiede, D. M.; Goshe, J. A.; Zuo, X.; Chen, L. X.; Barnard, A. S.; Zapol, P.; Curtiss, L.; Rajh, T. *Adv. Mater.* **2005**, *17*, 965. (b) Rabatic, B. M.; Dimitrijevic, N. M.; Cook, R. E.; Saponjic, Z. V.; Rajh, T. *Adv. Mater.* **2006**, *18*, 1033.

(4) Rajh, T.; Chen, L. X.; Lukas, K.; Liu, T.; Thurnauer, M. C.; Tiede, D. M. *J. Phys. Chem. B* **2002**, *106*, 10543.

(5) Dimitrijevic, N. M.; Saponjic, Z. V.; Bartels, D. M.; Thurnauer, M. C.; Tiede, D. M.; Rajh, T. *J. Phys. Chem. B* **2003**, *107*, 7368.

(6) Rajh, T.; Saponjic, Z.; Liu, J.; Dimitrijevic, N. M.; Scherer, N. F.; Vega-Arroyo, M.; Zapol, P.; Curtiss, L. A.; Thurnauer, M. C. *Nano Lett.* **2004**, *4*, 1017.

(7) Dimitrijevic, N. M.; Saponjic, Z. V.; Rabatic, B. M.; Rajh, T. *J. Am. Chem. Soc.* **2005**, *127*, 1344.

(8) Moore, T. A.; Gust, D.; Mathis, P.; Mialocq, J. C.; Chachaty, C.; Bensasson, L. *Nature (London)* **1984**, *307*, 630.

(9) Wasielewski, M. R.; Niemczyk, M. P.; Johnson, D. G.; Svec, W. A.; Minsek, D. W. *Tetrahedron* **1989**, *45*, 4785.

(10) Tommasi, L.; Shechter-Barloy, L.; Varech, D.; Battioni, J.-P.; Donnadieu, Q. B.; Verelst, M.; Bousseksou, A.; Mansuy, J. D.; Tuchagues J.-P. *Inorg. Chem.* **1995**, *34*, 1514.

(11) Eckert, T. S.; Bruice, T. C.; Gainor, J. A.; Weinreb, S. M. *Proc. Natl. Acad. Sci. U.S.A.* **1982**, *79*, 2533.

(12) (a) Itoh, S.; Huang, X.; Murao, H.; Komatsu, M.; Ohshiro, Y. J. *Inorg. Biochem.* **1993**, *51*, 87. (b) Itoh, S.; Komori, T.; Chiba, Y.; Ishida, A.; Takamuku, S.; Fukuzimi, S. *Chem. Commun.* **1996**, 465. (c) Itoh, S.; Kawakami, H.; Fukuzumi, S. *J. Am. Chem. Soc.* **1997**, *119*, 439. (d) Itoh, S.; Kawakami, H.; Fukuzumi, S. *J. Am. Chem. Soc.* **1998**, *120*, 7271.

(13) Wanner, M.; Sixt, T.; Klinkhammer, K.-W.; Kaim, W. *Inorg. Chem.* **1999**, *38*, 2753.

(14) (a) Katz, E.; Schlereth, D. D.; Schmidt, H.-L. *J. Electroanal. Chem.* **1994**, *367*, 59. (b) Katz, E.; Willner, I.; Kotlyar, A. B. *J. Electroanal. Chem.* **1999**, *479*, 64.

(15) (a) Duine, J. A. *Eur. J. Biochem.* **1991**, *200*, 271. (b) Anthony, C. *Arch. Biochem. Biophys.* **2004**, *428*, 2.

(16) Kuwabata, S.; Nishida, K.; Tsuda, R.; Inoue, H.; Yoneyama, H. *J. Electrochem. Soc.* **1994**, *141*, 1498.

(17) Rajh, T.; Tiede, D. M.; Thurnauer, M. C. *J. Non-Cryst. Solids* **1996**, *207*, 815.

(18) Lakshmi, K. V.; Reifler, M. J.; Brudvig, G. W.; Poluektov, O. G.; Wagner, A. M.; Thurnauer, M. C. *J. Phys. Chem. B* **2000**, *104*, 10445.

(19) (a) Noar, J. B.; Rodriguez, E. J.; Bruice, T. C. *J. Am. Chem. Soc.* **1985**, *107*, 7198. (b) Nakamura, N.; Kohzuma, T.; Kuma, H.; Suzuki, S. *Acta Crystallogr., Sect. C* **1993**, *49*, 2093. (c) Suzuki, S.; Sakurai, T.; Itoh, S.; Ohshiro, Y. *Inorg. Chem.* **1988**, *27*, 591.

(20) Zhu, Z.; Davidson, V. *Biochem. J.* **1998**, *329*, 175.

(21) Howe, R. F.; Graetzel, M. *J. Phys. Chem.* **1985**, *89*, 4495.

(22) Serpone, N.; Lawless, D.; Khairutdinov, R.; Pelizzetti, E. *J. Phys. Chem.* **1995**, *99*, 16655.

(23) Nozik, A. J.; Memming, R. *J. Phys. Chem.* **1996**, *100*, 13061.

(24) Colombo, D. P.; Bowman, R. M. *J. Phys. Chem.* **1996**, *100*, 18445.

(25) Veltwisch, D.; Janata, E.; Asmus, K. D. *J. Chem. Soc., Perkin Trans. 2* **1980**, 146.

(26) Eberhardt, M. K.; Colina, R. *J. Org. Chem.* **1988**, *53*, 1071.

(27) (a) Florin, R. E.; Brown, H. W.; Wall, L. A. *J. Phys. Chem.* **1962**, *66*, 2672. (b) Fessenden, R. W.; Schuler, R. H. *J. Chem. Phys.* **1963**, *39*, 2147.

(28) Howe, R. F.; Gratzel, M. *J. Phys. Chem.* **1987**, *91*, 3906.

(29) Micic, O. I.; Zhang, Y.; Cromack, K. R.; Trifunac, A. D.; Thurnauer, M. C. *J. Phys. Chem.* **1993**, *97*, 7277.

(30) Anpo, M.; Shima, T.; Fujii, T.; Suzuki, S.; Che, M. *Chem. Lett.* **1987**, 1997.

(31) Rajh, T.; Nedeljkovic, J. M.; Chen, L. X.; Poluetkov, O.; Thurnauer, M. C. *J. Phys. Chem. B* **1999**, *103*, 3515.

(32) Rajh, T.; Ostafin, A. E.; Micic, O. I.; Tiede, D. M.; Thurnauer, M. C. *J. Phys. Chem.* **1996**, *100*, 4538.

(33) Tae, E. L.; Lee, S. H.; Lee, J. K.; Yoo, S. S.; Kang, E. J.; Yoon, K. B. *J. Phys. Chem. B* **2005**, *109*, 22513.

(34) Elias, M. D.; Nakamura, S.; Migita, C. T.; Miyoshi, H.; Toyama, H.; Matsushita, K.; Adachi, O.; Yamada, M. *J. Biol. Chem.* **2004**, *279*, 3078.

(35) (a) Kay, C. M.; Mennenga, B.; Gorisch, H.; Bittl, R. *FEBS Lett.* **2004**, *564*, 69. (b) Kay, C. M.; Mennenga, B.; Gorisch, H.; Bittl, R. *J. Am. Chem. Soc.* **2005**, *127*, 7974.

(36) van de Lagemaat, J.; Kopidakis, N.; Neale, N. R.; Frank, A. J. *Phys. Rev. B* **2005**, *71*, 035304.

(37) Berger, T.; Sterrer, M.; Diwald, O.; Knozinger, E.; Panayotov, D.; Thompson, T. L.; Yates, J. T., Jr. *J. Phys. Chem. B* **2005**, *109*, 6061.

(38) Dominio, L. A. K.; MacCrone, R. K. *Phys. Rev.* **1967**, *156*, 910.

(39) (a) Turner, G. M.; Beard, M. C.; Schmuttenmaer, C. A. *J. Phys. Chem. B* **2002**, *106*, 11716. (b) Hendry, E.; Wang, F.; Shan, J.; Heinz, T. F.; Bonn, M. *Phys. Rev. B* **2004**, *69*, 081101.

(40) Kano, K.; Mori, K.; Uno, B.; Kubota, T.; Ikeda, T.; Senda, M. *Bioelectrochem. Bioenerg.* **1990**, *23*, 227

(41) She, C.; Anderson, N. A.; Guo, J.; Liu, F.; Goh, W.-H.; Chen, D.-T.; Mohler, D. L.; Tian, Z.-Q.; Hupp, J. T.; Lian, T. *J. Phys. Chem. B* **2005**, *109*, 19345.